Morphological properties, chemical composition, cancer risks and toxicological potential of airborne particles from traffic and urban background sites

Célia Alves, Ismael Casotti Rienda, Ana Vicente, Estela Vicente, Cátia Gonçalves, Carla Candeias, Fernando Rocha, Franco Lucarelli, Giulia Pazzi, Nora Kováts, Katalin Hubai, Casimiro Pio, Oxana Tchepel

PII: S0169-8095(21)00393-8

DOI: https://doi.org/10.1016/j.atmosres.2021.105837

Reference: ATMOS 105837

To appear in: *Atmospheric Research*

Received date: 8 May 2021

Revised date: 6 August 2021

Accepted date: 25 August 2021

Please cite this article as: C. Alves, I.C. Rienda, A. Vicente, et al., Morphological properties, chemical composition, cancer risks and toxicological potential of airborne particles from traffic and urban background sites, *Atmospheric Research* (2018), https://doi.org/10.1016/j.atmosres.2021.105837

Morphological properties, chemical composition, cancer risks and toxicological potential of airborne particles from traffic and urban background sites

Célia Alves[1], Ismael Casotti Rienda[1], Ana Vicente[1], Estela Vicente[1], Cátia Gonçalves[1], Carla Candeias[2], Fernando Rocha[2], Franco Lucarelli[3], Giulia Pazzi[3], Nora Kováts[4], Katalin Hubai[4], Casimiro Pio[1], Oxana Tchepel[5]

[1]Department of Environment and Planning, Centre for Environmental and Marine Studies (CESAM), University of Aveiro, 3810-193 Aveiro, Portugal

[2]Geobiosciences, Geotechnologies and Geoengineering Research Centre (GeoBioTec), Department of Geosciences, University of Aveiro, 3810-193 Aveiro, Portugal

[3]INFN - Firenze, National Institute for Nuclear Physics - Florence division, 50019, Sesto Fiorentino, Italy

[4]Centre for Environmental Sciences, University of Pannonia, Egyetem str. 10, Veszprém, 8200, Hungary

[5]Research Centre for Territory, Transports and Environment (CITTA), Department of Civil Engineering, University of Coimbra, Polo II, 3030-788 Coimbra, Portugal

Abstract

From a sampling campaign from December 2013 to June 2019, at a traffic and an urban background site in Coimbra, Portugal, two particulate matter (PM_{10}) samples from each month were selected to characterise the morphology by scanning electron microscopy, to determine the organic and inorganic chemical composition by multiple analytical techniques and to assess the ecotoxicity by the *Vibrio fischeri* bioluminescence inhibition assay. PM_{10} concentrations in winter were approximately twice as high as those recorded in the spring. Biomass burning was the greatest contributor to air pollution in winter at both sites. The contribution of vehicle emissions to the PM_{10} at the roadside was, on average, 7 times higher than at the background location. Distinct particle morphologies were observed. Higher abundances of aggregates enriched in Fe, Ti, Ba, Cr, Co, Cu, Zr, Mn and soot particles were registered in samples from the roadside. Bivariate plots suggested common sources of PAHs, mostly traffic and biomass burning, across the city. Benzo[a]pyrene equivalent concentrations were within the values documented for other European cities. Cancer risks resulting from exposure to PAHs by inhalation were estimated to be low ($10^{-6}\leq$ to $<10^{-4}$) for both sites. The noncarcinogenic risks from particulate trace elements were always higher than the target value of 1. Cancer risks for Cr were found to be higher than the acceptable level (10^{-6}). The calculation of toxic units indicated that 64% of the samples from the roadside location were toxic and 14% very toxic, while the corresponding shares for the urban background site were 50% and 7%, respectively. Many PM_{10}-bound constituents, especially markers of biomass burning (e.g. anhydrosugars) and traffic emissions (e.g. Fe, Cu, Zn), showed significant statistical correlations with toxicity.

Keywords: PM_{10}, PAH and alkyl-PAH, metals, morphology, cancer and non-cancer risks, ecotoxicity

Introduction

In 2019, air pollution was the 4th foremost risk factor for premature death around the world, exceeded only by hypertension, smoking, and poor eating habits. Globally, it was estimated to have caused 6.67 million deaths, about 12% of the total (HEI, 2020). Particulate matter (PM) is the major driver of global trends in the burden of disease ascribable to the air pollution cocktail (Cohen et al., 2017). Scientific results indicate that health outcomes can happen even at levels below standards (Kelly and Fussell, 2015; Makar et al., 2017; WHO, 2013). The underlying causes of the adverse effects are becoming better understood, but still far from being completely clarified, since the toxicology of the particulate material depends on its physicochemical properties, which vary with the meteorological conditions and emission sources of each region. In fact, there is heterogeneity in the toxic potency of the PM-bound components, some of which are essentially non-hazardous (e.g. sea salt), although they may represent a substantial mass fraction, while others, even present at very low levels, may pose very high risks (e.g. polycyclic aromatic hydrocarbons – PAHs, some metals). Primary combustion-derived particulate constituents seem to be especially important in causing inflammation and oxidative stress, which may describe most of the observed adverse health effects (Låg et al., 2020; Lomnicki et al., 2014; Muller, 2020; Wu et al., 2018).

Along with residential biomass combustion in many regions, one of the most important sources of PM, especially in urban areas, is road transport. Road vehicles sold in the European market and many other parts of the world must meet exhaust emission standards. After the launch of the Euro 5 and Euro VI standards for light-duty vehicles and for heavy-duty vehicles, respectively, the emission limits for particle number can only be reached by coupling diesel particulate filters. More recent requirements are also demanding the use of particulate filters on gasoline direct injection engines. Consequently, there has been a noticeable decay in the number and mass of road traffic related particles (Harrison, 2020). Non-exhaust emissions, which comprise particles from pavement abrasion, brake and tyre wear, and road dust resuspension, became a larger fraction of total road traffic emissions (AQEG, 2019; Padoan and Amato, 2018). The harmful impact of air pollution caused by diesel exhaust emissions on the human health is well known. However, recent researches have shown that non-exhaust particles may be just as damaging as exhaust fumes (Gerlofs-Nijland et al., 2019; Puisney et al., 2018; Selley et al., 2020). Given that non-exhaust particles have a different composition (e.g. higher metal concentrations) and size distribution from those emitted by vehicle exhausts, they also have distinctive toxicological properties (Grigoratos and Martini, 2014). Thus, up-to-date research should be conducted to better interpret the potential health risks of this aspect of vehicular pollution and to pave the way for further policy.

In Portugal, only a few studies have focused on PM monitoring programmes in urban environments. Almeida et al. (2009) collected aerosol samples for one year in the centre of Lisbon to analyse the ion and elemental contents. Almeida-Silva et al. (2020) and Almeida et al. (2005) performed short-term and 1-year long sampling campaigns in a traffic-impacted and a suburban location, respectively, in the outskirts of Lisbon, to identify the major sources based on the elemental composition. With the objective of identifying sources, Oliveira et al. (2010) measured the ionic and elemental composition of the fine and coarse aerosol at two distinct sites (roadside and urban background) in the city centre of Oporto, in short-term summer and winter campaigns. More recently, Custódio et al. (2016) and Pio et al. (2020) presented the results of one-year measurements of carbonaceous components, major ions, and elements in aerosols from an urban kerbside location in Oporto, and applied source apportionment methodologies. The only study focused exclusively on detailed organic speciation of aerosols sampled in a short-term campaign at two urban background sites in the outskirts of Oporto and in the city of Coimbra was documented by Alves et al. (2014). However, none of these studies encompassed the simultaneous characterisation of organic and inorganic constituents, nor an assessment of health risks or the toxicity of the particulate material.

To elucidate the role of PM in public health, and to contribute to a more effective management of air quality and to the design of pollution mitigation strategies in each region, it becomes necessary (i) a multi-component monitoring programmes, incorporating not only organic and inorganic constituents, but also morphological properties, since these can provide information on particle sizes, composition, shapes, aggregation, and even emission sources and formation processes, (ii) an improved understanding of the toxicological properties of PM and compounds that induce adverse effects, through an interdisciplinary strategy involving chemical characterisation, exposure bioassays and health risk assessment of multicomponent mixtures. To respond to these challenges, PM samples from a long-term sampling campaign at both roadside and urban background sites were selected to carry out a detailed physico-chemical characterisation and toxicological assessment. The complete datasets containing concentrations of carbonaceous constituents, major, minor and trace elements, and anhydrosugars will be used to apply and compare two source apportionment methodologies in an upcoming publication: positive matrix factorisation (PMF) and ion and mass balance (IMB). The present study additionally included the morphological properties of the particles and the analysis of about 35 PAHs and alkyl-PAHs, which, together with the elemental composition, were used to assess cancer and non-cancer risks via the inhalation route. With the objective of establishing concentration-response relationships or stressor-response patterns, a direct contact *in vitro* test was also applied to assess the (eco)toxicity of the aerosol samples.

Methodologies

Sampling

Particulate matter with equivalent aerodynamic diameter lower than 10 μm (PM_{10}) was simultaneously collected at a background location (Institute of Geophysics) and a traffic impacted site (University Stadium) in Coimbra, a city in central Portugal (Lat.: 40.2115, Long.: -8.4292) with an estimated population of about 140,000 inhabitants. The economy of the city mainly rests on its 35,000 higher education students and large hospital centres. Apart from an important cement factory located approximately 10 km to the north, there are no other large-scale nearby industries. The first sampling site was positioned in a residential area (urban background), while the second was placed in one of the university campuses, along a busy road giving access to shopping areas and the city centre (roadside). Samples were taken for 24 h, every 2 days, from 00:01 to 23:59 (local time). Two instruments were employed in parallel: i) a high-volume air sampler (MCV CAV-A/mb) equipped with pre-fired 15 cm diameter quartz fibre filters (Pall Corporation) and running at a flow rate of 30 m^3 h^{-1}, and ii) a low volume sampler (Echo PM Tecora) operating at 2.3 m^3 h^{-1} with 47 mm diameter Teflon filters (Pall Corporation). From the total set of samples, for each location, two filters for each month, more or less evenly spaced, were selected to make a more detailed physico-chemical and toxicological characterisation.

Analytical techniques

Gravimetric quantifications were carried out on an analytical balance (RADWAG 5/2Y/F) in a humidity-controlled room. The masses of each filter were determined from the average of 6 weighings (relative standard deviation < 0.02%). Two 9 mm circular portions from the quartz filters were cut to quantify the organic (OC) and elemental carbon (EC) content by a thermo-optical transmission technique, using the EUSAAR2 protocol (Pio et al., 2011). Two other portions of the quartz filters (4.7 cm diameter) were extracted by sonication with 75 mL of hexane/toluene (16:9), followed by concentration in a Turbo Vap® II evaporation system (Biotage) and drying under a nitrogen atmosphere. PAHs, alkylated PAHs and plasticisers were quantified by gas chromatography-mass spectrometry (Shimadzu, model QP5050A) equipped with a TRB-5MS 30 m × 0.25 mm × 0.25 μm column (Vicente et al., 2019). The analysis was accomplished by single ion monitoring (SIM) using a mixture of deuterated internal standards. Two 5 mm diameter punches were cut from each of the selected quartz filters. A Hitachi S-4100 scanning electron microscope (SEM) coupled to a Bruker Quantax 400 Energy Dispersive Spectrometer (EDS) was employed to perform the morphological characterisation of the particulate material. The identification of inorganic insoluble particles was performed using a mix of protocols that allowed to semi-quantify the mineralogy of each particle (Wu et al., 2016). Teflon filters were divided into two halves. One half was extracted ultrasonicated with 10 mL of ultra-pure Milli-Q water, followed by filtration through disposable syringe filter devices. Part of the water solutions were used for the determination of anhydrosugars and polyols in a high-

performance anion-exchange chromatographer with pulsed amperometric detection (HPAE-PAD) from Thermo Scientific™ Dionex™, model ICS-5000+, supplied with a Carbopac PA-1 guard column and a Carbopac PA-1 anion-exchange analytical column (Gonçalves et al., 2021). The remaining volume of the solutions was analysed by ion chromatography (Custódio et al., 2016). The other half of each Teflon filter was employed in the determination of major, minor and trace elements with Z > 10 by proton-induced X-ray emission (PIXE) (Lucarelli et al., 2018).

Estimation of PAH concentrations in the gas-phase

The concentration of PAHs in the gas phase was estimate in accordance with gas/particle (G/P) partitioning theory (Pankow, 1994a, b), as detailed by Gao et al. (2015) and Xie et al. (2013):

$$K_{p,OM} = \frac{K_p}{f_{OM}} = \frac{F/M_{OM}}{A} \quad (1)$$

$$K_{p,OM} = \frac{RT}{10^6 \overline{MW}_{OM} \xi_{OM} P_L^0} \quad (2)$$

$$A = \frac{10^6 \overline{MW}_{OM} \xi_{OM} P_L^0 F}{RT} \times \frac{1}{M_{OM}} \quad (3)$$

where,

$K_{p,OM}$ is the absorptive G/P partitioning coefficient of each polyaromatic; K_p is the G/P partitioning coefficient and f_{OM} is the weight fraction of the absorptive organic matter (*OM*) in the total PM; *F* and *A* represent the levels of each polyaromatic in the particle and gas phase, respectively (ng m^{-3}); M_{OM} and $\overline{MW}_{OM}$ are the concentrations of the particle-phase *OM* (μg m^{-3}) and the mean molecular weight (*MW*) of the absorbing *OM* phase (g mol^{-1}); *R* (m^3 atm K^{-1} mol^{-1}) is the ideal gas constant; *T* (K) is the ambient temperature; ξ_{OM} is the mole fraction scale activity coefficient of each compound in the absorbing *OM* phase; and p_L^0 (atm) is the vapour pressure of each pure compound. Values of ξ_{OM} were considered equal to 1 for all species, while $\overline{MW}_{OM}$ was assumed to be 200 g mol^{-1} (Xie et al., 2013; Gao et al., 2015). Vapour pressures were calculated as follows:

$$p_L^0 = p_L^{0,*} exp\left[\frac{\Delta H_{vap}^*}{R}\left(\frac{1}{298.15} - \frac{1}{T}\right)\right] \quad (4)$$

where $p_L^{0,*}$ and ΔH_{vap}^* are, respectively, the vapour pressure of each pure compound and the enthalpy of vaporisation (kJ mol^{-1}) at 298.15 K, and *R* is expressed in J mol^{-1} K^{-1}. The $p_L^{0,*}$ and ΔH_{vap}^* values

were obtained from Roux et al. (2008), Xie et al. (2013) and the Hazardous Substances Data Bank (HSDB, 2020). M_{OM} was considered as 2 times the OC (Gao et al., 2015).

Inhalation risk assessment

Noncarcinogenic and carcinogenic risks related to the inhalation of PM_{10}-bound elements in the outdoor air were calculated following the methodology of the United States Environmental Protection Agency (USEPA), and described in Alves et al. (2020a):

$$THQ = (EF \times ED \times ET \times C)/(R_fC \times AT) \quad (5)$$

$$TR = (EF \times ED \times ET \times C \times IUR)/AT \quad (6)$$

where THQ and TR are, respectively, the target hazard quotient and the target carcinogenic risk (unitless), EF is the exposure frequency (365 days a year), ED is the length of time during which a person is exposed to potentially hazardous constituents throughout life (70 years), ET is the exposure time (multiple time frames were considered, in p r day), C is the element concentration (mg m^{-3}), and AT is the averaging time (70 years, i.e. 613,2 h). R_fC is the reference concentration set by USEPA (mg m^{-3}; Table S1), which has not yet been established for some elements (USEPA, 2017, 2019). When necessary, R_fC values were derived from reference doses for oral exposure (R_fD, mg kg^{-1} day^{-1}), as follows (USEPA, 2013):

$$R_fC = (R_fD \times BW) / IR \quad (7)$$

where BW represents the body weight (70 kg) and IR is the average inhalation rate for an adult (20 m^3 day^{-1}). For carcinogenic elements, the chronic inhalation unit risk (IUR) values provided by USEPA (2017) were used: arsenic 4.3×10^{-3} ($\mu g\ m^{-3}$)$^{-1}$, lead 1.2×10^{-5} ($\mu g\ m^{-3}$)$^{-1}$, and hexavalent chromium 8.4×10^{-2} ($\mu g\ m^{-3}$)$^{-1}$. The IUR value for Cr(VI) evolved from a Cr(III):Cr(VI) share of 1:6. Given that in this work the total Cr concentration was determined, 1/7 of that value was used to estimate the risk. A THQ <1 suggests no significant or acceptable risk, a THQ > 1 indicates that noncarcinogenic effects are expected to occur, and a THQ > 10 reveals a high chronic risk. For carcinogens, USEPA considers that, when TR < 10^{-6}, exposure by inhalation to these constituents will not cause significant risks, but caution is suggested to guarantee that the collective cancer risk for all potential cancer inducers does not exceed 10^{-4} (Slezakova et al., 2014).

The carcinogenic risk of a PAH mixture is frequently expressed by its benzo[a]pyrene equivalent concentration (BaP_{eq}). BaP_{eq} concentrations are obtained by multiplying the levels of individual polyaromatics (PAH_i) in the gas and particulate phases by the respective toxicity equivalent factor (TEF_i), provided in the supplementary material (Table S2). The mutagenicity associated with BaP (BaP_{meq}) is estimated in the same way, replacing only TEF with mutagenic equivalency factors (MEF). The lifetime lung cancer risk was assessed through eq. (6), where C is ΣBaP_{eq}, and IUR is the inhalation unit risk of respiratory cancer for BaP_{eq}, which is 1.1×10^{-6} (ng m^{-3})$^{-1}$. The lifetime cancer risks have been categorised as (Roy et al., 2020): very low ($\leq10^{-6}$), low ($10^{-6}\leq$ to $<10^{-4}$), moderate ($10^{-4}\leq$ to $<10^{-3}$), high ($10^{-3}\leq$ to $<10^{-1}$), and very high ($\geq10^{-1}$)

Toxicology assessment

The kinetic version of the *Vibrio fischeri* bioluminescence inhibition bioassay was used to assess the ecotoxic potential of the samples. Contrary to other common tests, the bulk samples are tested without prior solvent extraction, simulating a realistic exposure pathway that happens between the particles and the recipient organisms. The bioassay rests on the inhibition of the NAD(P)H:FMN oxidoreductase and luciferase enzyme system. The decrease in light emittance of the bacterium is proportional to the strength of the toxicants. Quartz filter punches of 19 mm in diameter were cut and ground in an agate mortar. After transferring into pre-cleaned 4 mL vials, 2 mL of high-purity (Milli-Q) water were added with continuous stirring. The suspensions were tested following the protocol of Kováts et al. (2012), which is based on the ISO 21338:2010 standard. Luminometric measurements of the bacterial suspensions were made in a Thermo Luminoscan Ascent unit. Ecotoxicity (EC_{50}) of each sample was calculated as the mass of particle-bound constituents that causes a 50% decrease in bioluminescence when compared to the control. The lower is the EC_{50} value, the higher is the ecotoxicity of the particulate matter samples. The Ascent Software from Aboatox Co., Finland, was used to calculate the EC_{50} values. Toxic Units ($TU=100/EC_{50}$) were determined as a measured of toxicity in each sample. Based on TU values, distinct toxicity levels can be considered (Chang et al., 2013): TU < 1 non-toxic, 1 < TU < 10 toxic, 10 < TU < 100 very toxic and TU > 100 extremely toxic.

Statistical analysis

The Shapiro-Wilk normality tests was used to assess if the data set could be modelled by a normal distribution. To assess the homoscedasticity of variances, the Levene's test was applied. Since variables were not normally distributed, the non-parametric Spearman rank correlation method was followed. All statistical analyses were performed with the IBM SPSS Statistics software, version 24.

Results and discussion

Chemical mass balance of PM_{10} and sources

To perform a PM_{10} mass balance (Fig. 1), the concentrations of the elements were stoichiometrically converted into their most frequent oxides (e.g. SiO_2, Fe_2O_3, Al_2O_3, CaO, Na_2O, MgO, K_2O, TiO_2). At the roadside, organic matter, elemental carbon, nitrate, ammonium, and element oxides accounted, on average, for 37.6, 12.3, 5.9, 1.1 and 33.6%wt. of the PM_{10} mass, respectively. A lower EC mass fraction (6.3%wt.) was obtained in the background samples, while the proportion of OM was identical in both locations. Element oxides represented another major fraction (32.3%) in PM_{10} from this residential site, whereas secondary ions contributed to a lower share (nitrate – 7.5%wt., ammonium – 2.0%wt.). In addition to sampling and analysis artefacts, the unaccounted mass in the chemical mass balance can, at least in part, be due to unanalysed constituents. Besides, part of the unaccounted mass is generally allocated to particle-bound water.

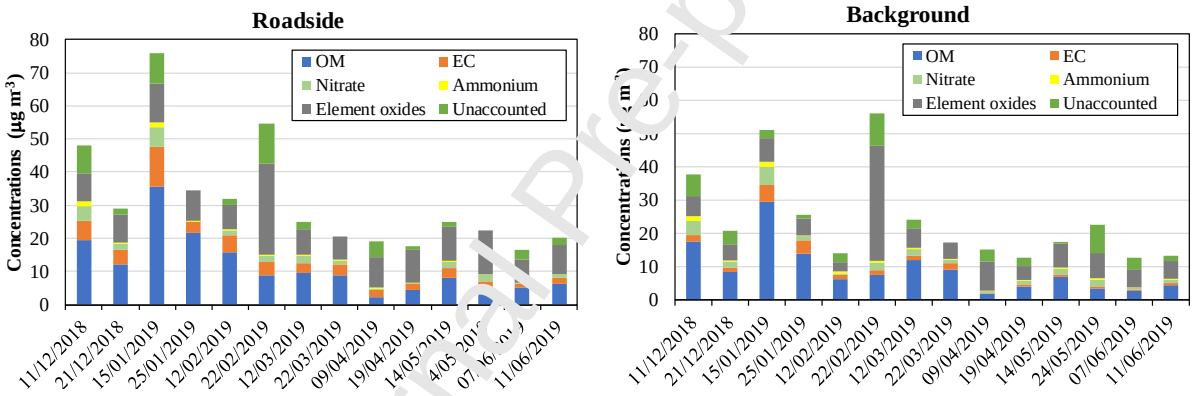

Fig. 1. Chemical mass balance of PM_{10}.

PM_{10} concentrations in winter were approximately twice as high as those recorded in the spring. Increased emissions in the coldest season, combined with the lower height of the atmospheric boundary layer and higher stability, lead to build-up of air pollutant concentrations. On January 15 and February 22, exceedances were registered to the daily limit value of 50 µg m^{-3} imposed by the Directive 2008/50/EC on ambient air quality. Backward trajectories (not shown), calculated by the Hybrid Single-Particle Lagrangian Integrated Trajectory (HYSPLIT) modelling system, indicated a Saharan dust intrusion on February 22, which has contributed to a high amount of crustal material in PM_{10}. During this episode, the concentrations of Fe, Al, Si and Ca at the roadside location increased, on average, 3.2, 5.1, 6.2 and 5.7 times, respectively, compared with the remaining days, whereas the corresponding rises in the urban background site were 15.0, 58.4, 47.3 and 5.2. On this day, very close Si/Al ratios were recorded in both locations: 2.14 and 2.17 at the urban background and roadside, respectively. These values are typical of a mixture of quartz and aluminosilicates (feldspar and clay minerals), which is characteristic of the Sahara (Marconi et al., 2014).

January 15th was one of the coldest days of the year. On this day, a significant increase in carbonaceous matter was observed, most likely due to residential wood combustion for heating. Biomass burning was estimated to account for a PM_{10} mass fraction of about 70% on this specific day. In fact, this source was the greatest contributor to air pollution in winter (Fig. 2), representing PM_{10} mass fractions of 30.2% and 43.1%, on average, at the roadside and background sites. At the roadside, vehicle emissions accounted for 24.4%wt. of PM_{10} in winter, but the contribution declined to 13.8% in spring samples, for which the influence of Atlantic air masses was reflected in an increased supply of fresh and aged sea salt. Sea spray is enriched in marine ions Na^+, Mg^{2+} and Cl^-, but during aging processes, chloride is depleted and sea salt aerosol in the form of $NaNO_3$ and/or Na_2SO_4 is formed. Regional and long-range transport of mineral dust contributed to mean mass fractions of 16.2% and 21.9% in winter samples, respectively, from the traffic impacted and urban background locations, mainly due to the aforementioned intrusion of Saharan origin. If this event is excluded from the calculations, the input of this source in winter is reduced to values more close to those obtained in the hottest period (roadside - 2.42%wt. in winter, 7.5%wt. in spring; background - 3.3%wt. in winter, 7.2%wt. in spring). Secondary inorganic aerosol formation accounted for about 5-6%wt. of the PM_{10}, both in winter and spring samples from the traffic impacted site. More pronounced photochemical aging processes contributed to greater shares in the urban background atmosphere (8.7%wt. in winter, 13.0%wt. in spring).

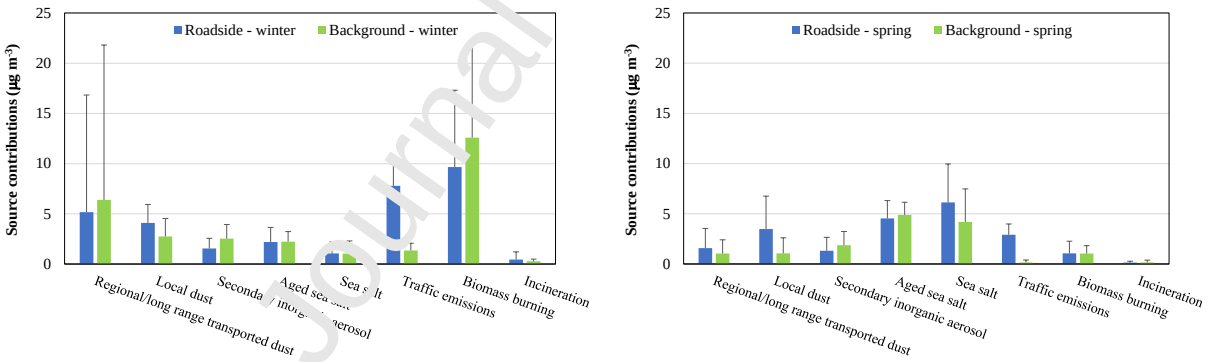

Fig. 2. Contributions of each individual source category to the total PM_{10} mass concentrations apportioned by PMF for the selected samples.

Morphological characterisation

The analysis of filters by SEM/EDS revealed the presence of particles with both natural (e.g. dust, soil resuspension and bioaerosols) and anthropogenic origin (e.g. soot). Diverse morphologies were observed, from individual particles to agglomerates with rounded to sharp shapes, as is the case of salts. The semiquantitative chemical analyses showed the presence of metals in many of the individual particles analysed.

A high abundance of aggregates enriched in Fe, Ti, Ba, Cr, Co, Cu, Zr, Mn and soot particles were found in samples from the roadside, reflecting the anthropogenic influence of urban-traffic sources (Fig. 3). In late February, a much higher content of Fe and other metal oxides were found in relation to other sampling periods, and especially when compared to a blank filter (Fig. S1, S2). The content and morphology of particles in early February were clearly distinct between locations, while in late February the Sahara intrusion was felt in a transversal way, making the characteristics of the samples comparable. Particle sizes at both sites in early February were visibly smaller (PM_5 or lesser), with rounded morphology, and identifiable pollen grains (from < 5 µm to larger sizes), reflecting the influence of nearby parks. During the Saharan dust intrusion, particles were distinctly larger, presenting a sharper morphology.

A greater abundance of soot particles was observed in samples from the roadside location (Fig. 3 and 4), reflecting the proximity to roads of more intense traffic. Soot particles are generally by-products of incomplete combustion at high pressures and temperatures in internal combustion engines (He et al., 2021).

In January, large amounts of fly ashes were detected in both sampling sites, with a probable origin in residential combustion of wood and/or coal (Fig. S3). As a result of the prevalence of air masses originating in the Atlantic, sea salt (NaCl) particles were found mostly in spring in both locations. Higher concentrations of highly Fe, Cr, Cu, Sn, Zr enriched clusters in roadside samples when compared to background location were also observed (Fig. S4).

Both sites are close to parks with dense vegetation. Several pollen grains and spores were found (Fig. S5). Pollens of Betulaceae and Cupressaceae trees have been considered a major cause of allergies and, conceivably, asthma symptoms worldwide (Stas et al., 2021; De Linares et al., 2021). Due to climate change, the concentrations and period of exposure to these pollens have been increasing over the years, contributing to aggravate health outcomes.

The identified inorganic particles, due to their chemical composition and morphology, may pose a health concern. Health-related injuries in lung cells exposed to dust extracts has been linked to the production of reactive oxygen species (ROS), mitochondrial lipid peroxidation, mitochondrial dysfunction, and cellular antioxidant imbalance (Pardo et al., 2017). Iron-catalysed free radical generation is recognised as a mechanism that boosts acute lung inflammation. Exposure of the lungs to mineral aerosol causes high oxidative damage due to the high oxygen levels and the presence of catalytically active iron in atmospheric particulate matter. Iron in the lungs can be a vehicle for microbial growth and replication, leading to more virulent and enduring infections (Nickovic et al., 2012).

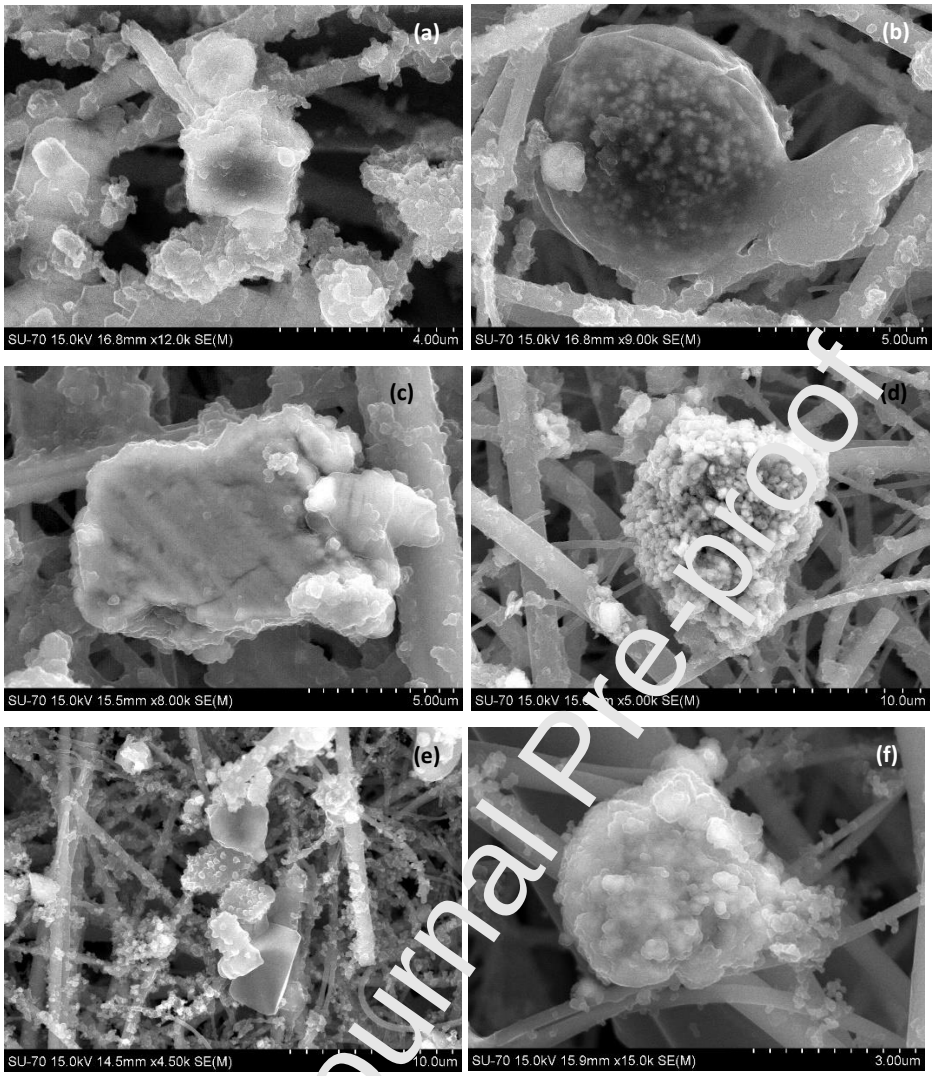

Fig. 3. SEM images of roadside samples: (a) Fe, Cu, Ba, Al rich aggregates; (b) Ti oxide in the centre; (c) Fe oxide; (d) metal oxide Fe, Cu, Ba, Al rich aggregate; (e) Fe oxides with salt and soot particles; (f) Fe, Cu, Zn rich aggregate and soot.

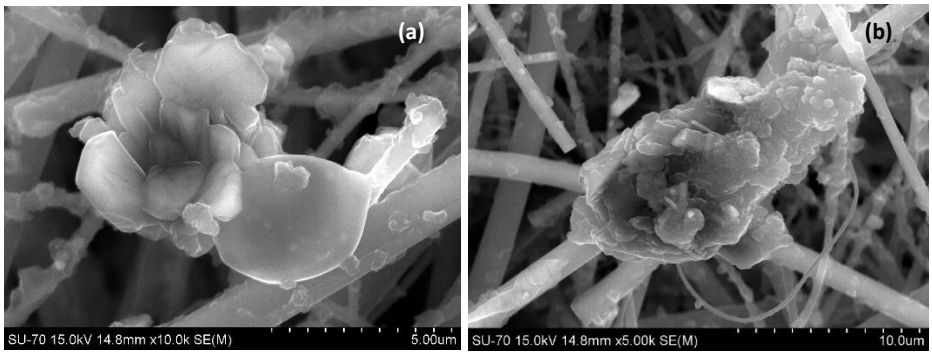

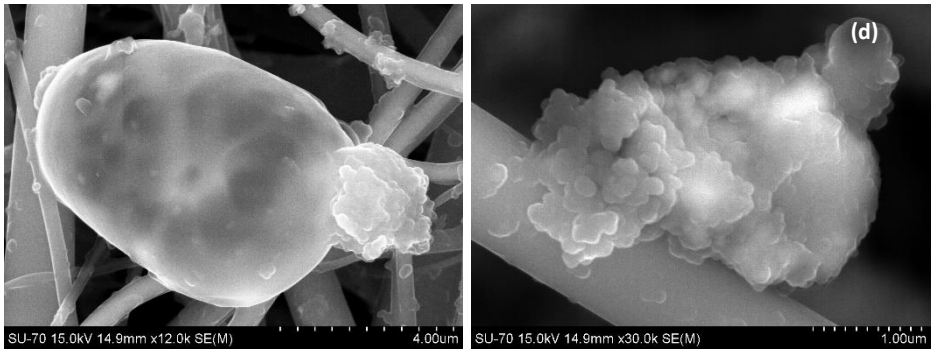

Fig. 4. SEM images of samples from the background site: (a) gypsum aggregate (top left) and rounded quartz particle; (b) An Al, S, Fe rich aggregate + soot; (c) Si-O-Al particle (centre) probably having suffered fragmentation/melting processes in e.g., engines, and NaCl aggregate (right); (d) Fe oxide.

Polycyclic aromatic hydrocarbons

The total mean concentrations of PAHs and alkyl-PAHs (gas + particle phases) determined in this work were 586 ng m^{-3} and 324 ng m^{-3} at the roadside and background site, respectively. The complete list can be found in the supplementary material (Tables S3 and S4). As expected, due to their volatility, an overwhelming proportion of 3-ring PAHs was estimated to be in the gas phase (Fig. 5). The mass percentages of PAHs in the gas phase decrease with increasing molecular weights. At the urban background site, gas phase 4-ring PAHs accounted for 56.5% of the total concentrations, on average, while 5- and 6-ring compounds were predominantly in the particulate phase. In the PM_{10} samples from the roadside location, 4- and 5-ring congeners in the gas phase represented 53.3% and 1.3% of total concentrations, whereas heavier compounds (indeno[1,2,3-cd]pyrene and benzo[g,h,i]perylene) were exclusively in the particulate phase.

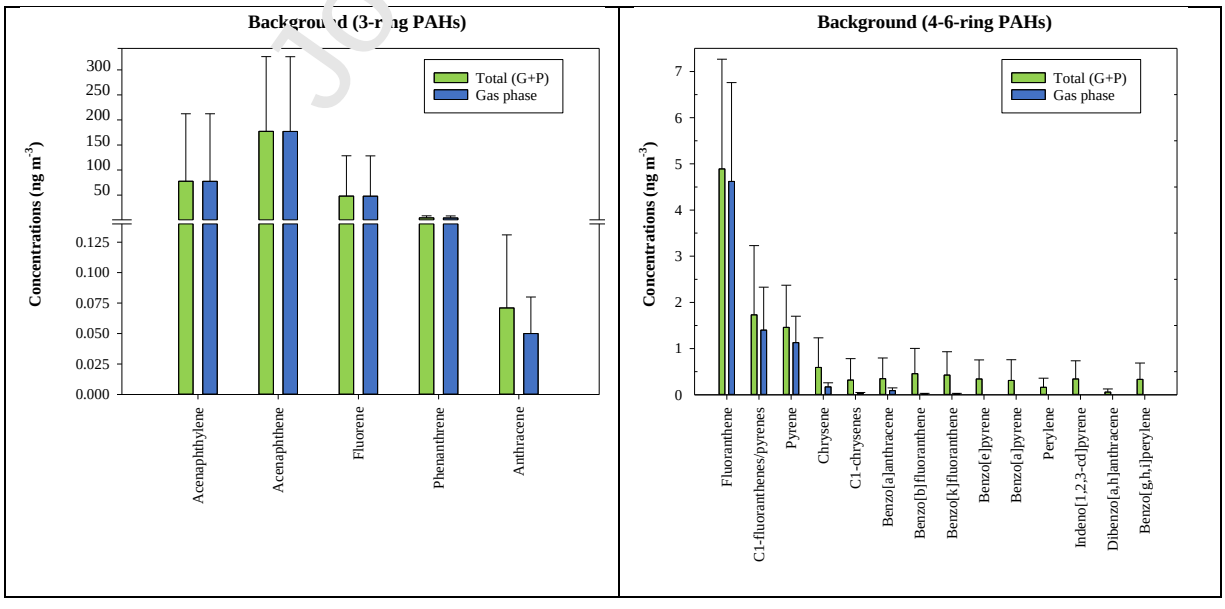

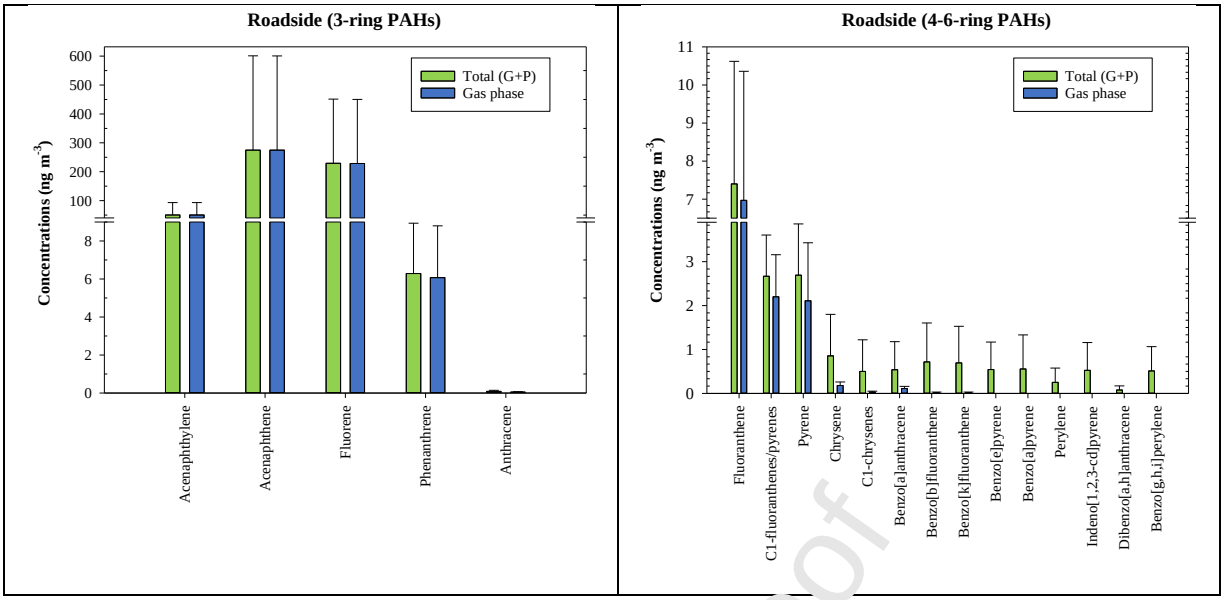

Fig. 5. Total concentrations of PAHs and alkyl-PAHs (sum of the gas and particulate phases) and only in the gas phase.

PAHs are generally formed by incomplete combustion of carbon-containing fuels. Bivariate plots have been used to investigate their sources. As most of the source profiles are only available for particulate phase PAHs, in the analysis of correlations (Fig. 6), only this phase was taken into account. One aspect that stands out when inspecting the graphs is the alignment between the concentrations of the samples from the roadside and those of the urban background atmosphere. This suggests common sources or mechanisms throughout the city. The scatter plots of Phen versus Ant present a significant deviation from the line that represents the typical emission profile for the most representative woody species and residential combustion equipment in Portugal, indicating that biomass burning was not the dominant source of these compounds. Although closer to the profile obtained in a road tunnel with circulation representative of the Portuguese vehicle fleet, the environmental data reflect higher proportions of Phe in relation to Ant, suggesting atmospheric aging processes. Anthracene is less stable than its isomeric kinked phenanthrene. As compared to anthracene, phenanthrene has a higher ionisation potential and a reduced electron affinity, which gives it a higher kinetic and thermodynamic stability (Poater et al., 2018). Likewise, despite the environmental data of BaA and Chr approaching the emission profile of biomass burning, there is a shift towards higher Chr concentrations. This is probably the result of a greater photochemical decay of BaA, since this PAH is more susceptible to reactions with atmospheric oxidants, such as ozone, than its isomer (Perraudin et al., 2007). The concentrations of Flu versus Pyr and BghiP versus IcdP are aligned with the emission profile of residential firewood combustion, pointing to a pyrogenic origin of these compounds. On the other hand, the scatter plots of BbF versus BkF and BeP versus

BaP overlap the on-road chemical fingerprint, indicating that they were mainly derived from traffic-related emissions.

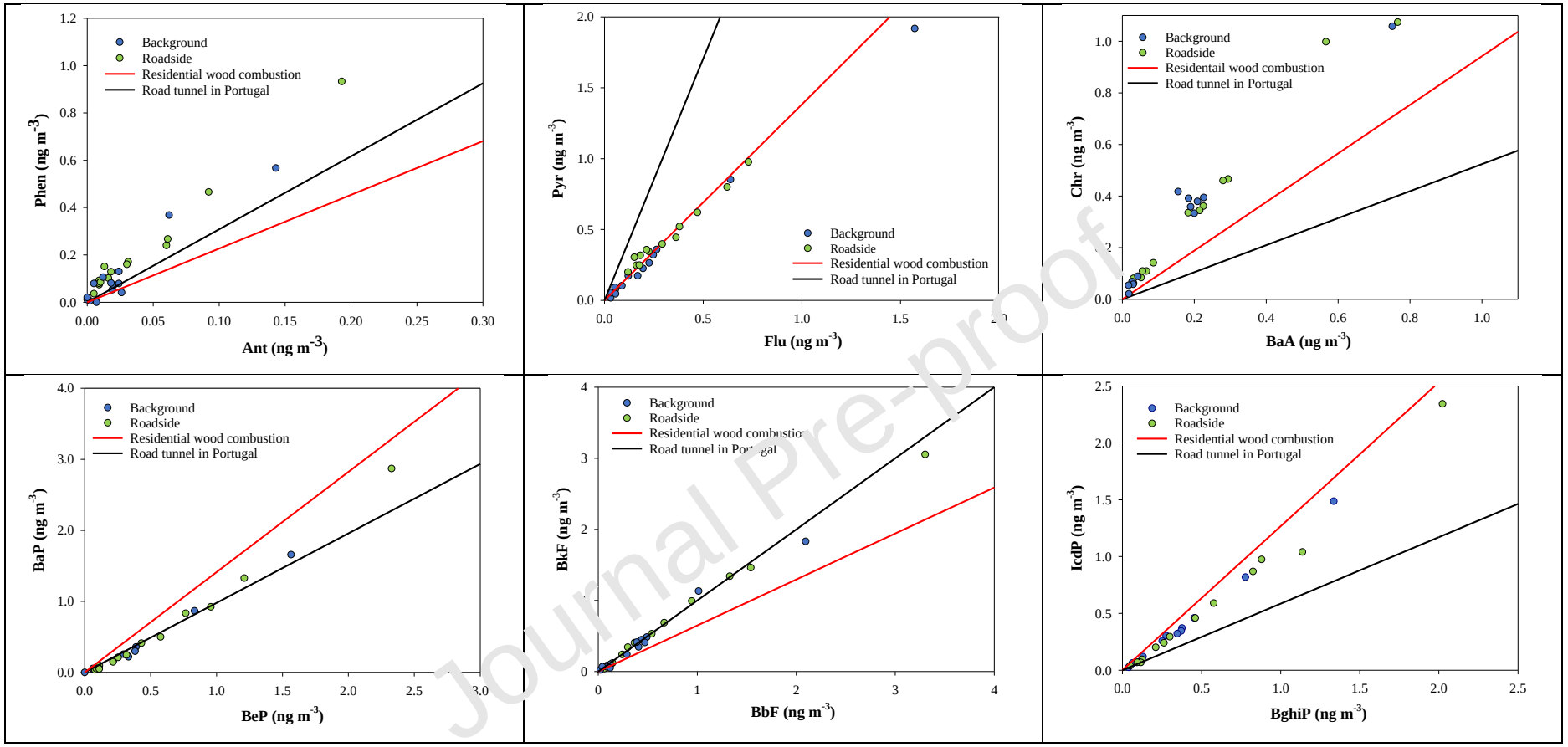

Fig. 6. Correlations between PAH congeners. Ant – anthracene, Phen - phenanthrene, Flu – fluoranthene, Pyr – pyrene, BaA – benzo [a]anthracene, Chr – chrysene, BeP – benzo[e]pyrene, BaP – benzo[a]pyrene, BbF – benzo[b]fluoranthene, BkF – benzo[k]fluoranthene, BghiP – benzo[g,h,i]perylene, IcdP – indeno[1,2,3-cd]pyrene. Data for residential biomass burning and road tunnel were taken from Gonçalves et al. (2011) and Alves et al. (2016), respectively.

Health risk assessment

Due to the usual lack of time-activity patterns for different microenvironments, one of the most common exposure assessment methods that has been used in epidemiology considers that ambient concentrations are representative of the total population exposure (Kazakos et al., 2020). Thus, when estimating cancer risks, outdoor levels are taken as a surrogate of daily 24 h exposure.

The noncarcinogenic risks associated with inhalation exposure to particulate trace elements were always > 1 (Table 1), indicating that health effects are likely to manifest. The highest values were recorded on February 22, the day of the Sahara dust intrusion. While on other days silica represented, on average, 14.5% and 13.3% of ΣTHQ, during the intrusion this contribution rose to 37.8% and 35.4% at the background and roadside locations, respectively. If outdoor levels are not taken as a surrogate of daily 24 h exposure, only partial exposures to the outdoor air < 4.9 h (roadside) and 5.6 h (background) would guarantee values ΣTHQ < 1. The target carcinogenic risks were estimated to be, in general, between 10^{-6} and 10^{-4}. These values, while not alarming, suggest that the risks are not negligible and that the adoption of measures is needed to avoid the development of new oncogenic cases due to cumulative exposure to cancer-triggering metals. Cancer risks are mostly due to Cr, with contributions to ΣTR around 98%. Cancer risks for Cr were previously found to be higher than the acceptable level (10^{-6}) in Athens and Lisbon (Chalvatzaki et al., 2019).

Table 1. Target hazard quotient (THQ) for noncarcinogenic constituents and target carcinogenic risk (TR) related to the inhalation to airborne PM_{10} metals.

	Roadside			Background		
	Avg	Min	Max	Avg	Min	Max
ΣTHQ	4.91	2.27	11.7	4.30	1.70	14.9
TR Cr	2.67×10^{-4}	4.27×10^{-5}	5.67×10^{-4}	2.88×10^{-4}	2.63×10^{-5}	1.32×10^{-3}
TR As	5.13×10^{-6}	7.02×10^{-7}	1.09×10^{-5}	3.98×10^{-6}	1.48×10^{-6}	7.73×10^{-6}
TR Pb	2.91×10^{-8}	1.27×10^{-8}	1.27×10^{-7}	1.43×10^{-8}	4.01×10^{-9}	3.66×10^{-8}
ΣTR	2.72×10^{-4}	4.35×10^{-5}	5.73×10^{-4}	2.92×10^{-4}	2.83×10^{-5}	1.33×10^{-3}

Total BaP_{eq} concentrations of 1.52±1.07 ng m^{-3} and 0.883±0.716 ng m^{-3} were obtained at the roadside and background locations, respectively. These levels are within the values documented for other European cities, but lower than those registered in Chinese and Indian megacities (Table 2). In PM_{10} from the background location, the compounds that contributed most to the ΣBaP_{eq} were acenaphthene (28.1%), benzo[a]pyrene (28.0%) and dibenzo[a,h]anthracene (6.5%). At the roadside, total BaP_{eq} concentrations were dominated by benzo[a]pyrene (29.2%), followed by acenaphthene

(22.4%) and fluorene (19.1%). Mutagenic compounds represented ΣBaP_{meq} of 16.3±1.49 ng m^{-3} at the roadside site, with benzo[a]pyrene, benzo[b]fluoranthene and indeno[1,2,3-cd]pyrene accounting for 42.3, 16.8 and 14.3% of total concentrations, respectively. At the background location, these PAHs held 26.7, 12.2 and 11.0% shares of ΣBaP_{meq} (9.82±0.901 ng m^{-3}), respectively.

On average, 1.67 and 0.971 cancer cases per million people from the inhalation of PAHs were estimated for the roadside and background sites, respectively (Table 2). These lifetime excess lung cancer risks are lower than those reported for other cities around the world, especially in overpopulated metropolises. Although low cancer risks have been estimated for both sites ($10^{-6}\leq$ to $<10^{-4}$), measures to mitigate the emission of main contributors to the total carcinogenic potential is recommended. Considering the exposure to ambient air as partial and dependent on the time spent outdoors, the associated cancer risks were calculated for various ET values. From this exercise, the following correlations were obtained: cancer risk = $(7\times10^{-8})\times$ET (roadside) and cancer risk = $(4\times10^{-8})\times$ET (background). These relationships allow us to conclude that the lifelong acceptable risk of 10^{-6} resulting from partial exposure to outdoor air is only exceeded for ET > 14.3 h/day for the roadside, while the target is never surpassed at the background location.

Table 2. Mean benzo[a]pyrene equivalent concentrations and lifetime cancer risks for daily 24 h exposures.

Location	ΣBaP_{eq} (ng m^{-3})	Cancer risk			Reference
		Average	Min	Max	
Coimbra, roadside, Portugal	1.52	1.67×10^{-6}	5.71×10^{-7}	5.22×10^{-6}	This study
Coimbra, background, Portugal	0.88	9.71×10^{-7}	1.20×10^{-7}	3.28×10^{-6}	This study
Oporto, Portugal	2.37	2.61×10^{-6}	4.40×10^{-7}	1.58×10^{-5}	Alves et al. (2017)
Florence, Italy	1.01	1.10×10^{-6}	5.42×10^{-7}	2.31×10^{-6}	Alves et al. (2017)
Athens, Greece	0.30	8.80×10^{-5}	4.29×10^{-5}	1.83×10^{-4}	Alves et al. (2017)
Central New Delhi, India: - Rajghat - Mayur Vihar - Mithapur	 21.0 27.5 32.3	2.34×10^{-5}			Sarkar and Khillare (2013)
New Delhi, India	13.9 (winter) 1.4 (summer)	4.23×10^{-4}	1.02×10^{-4} (semi urban)	7.88×10^{-4} (urban industrial-cum-residential)	Yadav et al. (2020)
Xi'an, China	17.0	1.8×10^{-5}	1.7×10^{-6}	7.0×10^{-5}	Bandowe et al. (2014)
Beijing, China	1.47	7.0×10^{-5}			Elzein et al. (2020)
New Delhi, India	3.42	7.0×10^{-5}			Elzein et al. (2020)

Toxicological potential of particulate matter

The TU index indicated that 64% of the samples from the roadside location were toxic and 14% very toxic, while the corresponding shares for the urban background site were 50% and 7%, respectively. The highest toxicities were recorded in the winter samples (Fig. 7), largely due to the significant contribution of biomass burning for residential heating. In fact, together with traffic emissions, biomass burning was the source whose mass contributions to PM_{10} most significantly inhibited light production by *V. fischeri*, which is considered a proxy of cellular toxicity (Table 3). Many negative correlations, indicating a decrease in EC_{50} (higher toxicity) with increasing compound concentrations, were found. Carbonaceous constituents and anhydrosugars were inversely correlated with EC_{50}, evidencing the hazardous effects of biomass burning emissions. Good relationships were established with xylitol. This polyol correlated very well with levoglucosan, suggesting a common origin in residential firewood combustion. Two plasticisers, bis(2-ethylhexyl) adipate (DEHA) and bis(2-ethylhexyl) phthalate (DEHP), were also able to elicit acute toxic effects. Although tyres may represent a substantial source of plasticisers into the atmosphere, these two compounds have been detected as minor constituents in particles resulting from the wear of this vehicle components (Alves et al., 2020b), suggesting an association with other microplastics that nowadays are spread everywhere. According to the International Agency for Research on Cancer (IARC), DEHA has not been labelled as carcinogenic to humans (Group 3), while DEHP is included in Group 2B (probable carcinogen). However, many studies have described the presence of reactive oxygen species (ROS), which cause oxidative stress in living systems containing these plasticisers. Insults occur not only to liver, but also to various organs, such as the central nervous, reproductive, pulmonary, and immune systems (Kovacic, 2010). The high toxicity of the vast majority of PAHs and alkylated PAHs was confirmed by the significant relationships for a 99% confidence level. Benzothiazole was significantly correlated at the 99% confidence level with EC_{50} only for samples from the more heavily trafficked site. This organic heterocyclic compound is a common component of tyre treads and has earlier been proposed as tracer for tyre wear (Asheim et al., 2019; Zhang et al., 2018). Strong correlations involving elements from both exhaust and non-exhaust traffic emissions, such as K, Cr, Mn, Fe, Cu, As and Pb (Alves et al., 2015a,b), were obtained. Zn showed a significant relationship with the toxicological response only for the roadside. Tyre wear has been described as an important source of Zn into the atmosphere (Alves et al., 2020b). For both locations, bivariate correlations between some ionic species and EC_{50} values were statistically significant, but positive, suggesting a decreasing toxic effect with increasing concentrations. In previous studies, it was also observed that innocuous water-soluble salts and other chemical species did not induce toxicological responses in different bioassays (Arif et al., 2017; Kasurinen et al., 2017; Totlandsdal et al., 2014).

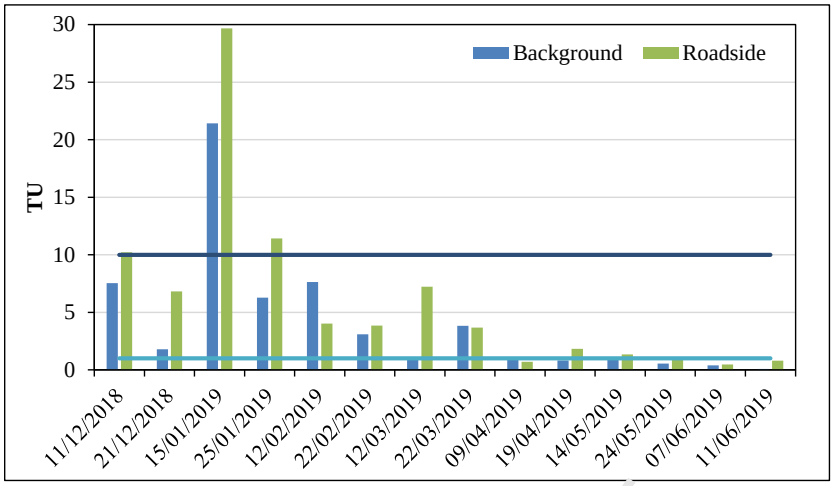

Fig. 7. Toxic units for the various samples of the urban background and roadside locations in Coimbra. Horizontal lines delimit the toxicity classes: non-toxic (< 1), toxic (between 1 and 10) and very toxic (> 10).

Table 3. Spearman correlation coefficients between a) PM_{10}-bound constituents and b) source contributions, and EC_{50} values (µg L^{-1}) from the *V. fischeri* biossay.

	Roadside (N=14)	**Background** (N=14)
PM_{10} (µg m^{-3})	-0.675**	-0.503
Carbonaceous compounds (µg m^{-3})		
OC	-0.859**	-0.692**
EC	-0.771**	-0.851**
TC	-0.864**	-0.723**
Water soluble ions (µg m^{-3})		
Chloride	0.437	0.719**
Nitrate	-0.345	-0.240
Sulfate	0.020	0.209
Sodium	0.317	0.785**
Ammonium	-0.273	-0.477
Potassium	-0.508	-0.319
Magnesium	0.112	0.846**
Calcium	-0.222	-0.746**
Metals (µg m^{-3})		
Na	0.613*	0.820**
Mg	0.644*	0.745**
Al	-0.007	-0.367
Si	-0.051	-0.376
P	-0.314	-0.468
S	-0.099	0.310
Cl	0.433	0.648*
K	-0.763**	-0.640*
Ca	-0.204	-0.464
Ti	-0.200	-0.407

V	-0.213	0.095
Cr	-0.587*	-0.569*
Mn	-0.618*	-0.657*
Fe	-0.604*	-0.653*
Ni	-0.310	-0.147
Cu	-0.785**	-0.811**
Zn	-0.763**	-0.477
As	-0.758**	-0.582*
Se	-0.125	-0.451
Br	-0.077	-0.033
Rb	-0.543*	-0.341
Sr	-0.429	-0.218
Y	-0.429	-0.191
Zr	-0.200	0.349
Mo	-0.081	0.449
Ba	-0.200	-0.213
Pb	-0.789**	-0.618*
Saccharides (μg m^{-3})		
Xylitol	-0.600*	-0.555*
Arabitol	-0.235	-0.020
Levoglucosan	-0.609*	-0.550*
Mannitol	-0.103	-0.108
Mannosan	-0.735**	-0.563*
Galactosan	-0.538*	-0.600*
PAHs and alkyl-PAHs (ng m^{-3})		
Benzothiazole	-0.754**	0.046
Carbazole	-0.650*	-0.500
p-Terphenyl	-0.679**	-0.745**
Retene	-0.833**	-0.928**
Naphthalene	-0.490	-0.508
C1-naphthalenes	-0.486	-0.367
C2-naphthalenes	-0.582*	-0.468
C3-naphthalenes	-0.618*	-0.387
C4-naphthalenes	-0.730**	-0.780**
Acenaphthylene	-0.675**	-0.247
Acenaphthene	-0.288	-0.521
Fluorene	-0.024	-0.178
C1-fluorenes	-0.700**	-0.754**
C2-fluorenes	-0.789**	-0.780**
Phenanthrene	-0.873**	-0.451
C1-phenanthrenes	-0.855**	-0.582*
Anthracene	-0.798**	-0.453
Fluoranthene	-0.829**	-0.789**
C1-fluoranthenes/pyrenes	-0.758**	-0.618*
C2-fluoranthenes/pyrenes	-0.869**	-0.789**
Pyrene	-0.798**	-0.833**
Chrysene	-0.851**	-0.697**
C1-chrysenes	-0.837**	-0.747**
C2-chrysenes	-0.853**	-0.464

C3-dibenzothiophenes	-0.851**	-0.780**
C4-dibenzothiophenes	-0.780**	-0.930**
Benzo[a]anthracene	-0.851**	-0.842**
7,12-Dimethylbenz[a]anthracene	-0.884**	-0.889**
Benzo[b]fluoranthene	-0.886**	-0.745**
Benzo[k]fluoranthene	-0.868**	-0.771**
Benzo[e]pyrene	-0.886**	-0.749**
Benzo[a]pyrene	-0.886**	-0.776**
Perylene	-0.859**	-0.673**
Indeno[1,2,3-cd]pyrene	-0.899**	-0.802**
Dibenzo[a,h]anthracene	-0.868**	-0.737**
Benzo[g,h,i]perylene	-0.873**	-0.815**
Plasticisers (ng m^{-3})		
Dimethyl phthalate	-0.133	0.338
Diethyl phthalate	0.305	-0.129
Diisobutyl phthalate	0.512	0.249
Di-n-butyl phthalate	0.366	0.272
Benzyl butyl phthalate	0.232	0.619*
Bis(2-ethylhexyl) adipate	-0.705**	-0.640*
Bis(2-ethylhexyl)phthalate	-0.727**	-0.780**
Source contributions (µg m^{-3})		
Regional/long range transported dust	0.031	-0.196
Local dust	-0.253	-0.727**
Secondary inorganic aerosol	-0.006	0.024
Aged sea salt	0.571*	0.701**
Sea salt	0.473	0.727**
Traffic emissions	-0.780**	-0.871**
Biomass burning	-0.605*	-0.701**
Incineration	-0.451	-0.253

**. Correlation is significant at the 0.01 level (2-tailed).

*. Correlation is significant at the 0.05 level (2-tailed).

Conclusions

In a PM_{10} sampling campaign carried out at a roadside and at an urban background station in Coimbra, Portugal, much higher concentrations were registered in winter, mainly due to residential biomass combustion. One exceedance of the air quality limit was attributed to a Saharan dust intrusion, which caused a sharp rise in Fe, Al, Si and Ca levels. The identified particles showed a sharper morphology at both locations during this event, when compared to other sampling periods. Concentrations of PAHs and alkyl-PAHs were approximately twice as high at the site most impacted by traffic than at the background station. It was estimated that an overwhelming proportion of 3-ring PAHs was in the gas phase, while 5-6-ring compounds were mostly partitioned into the particulate phase. The gas phase of the 4-ring congeners represented 53-57% of the total concentrations. Biomass burning and traffic emissions were identified as the major sources of PAHs, although atmospheric

aging processes due to photochemical decay may have affected the concentrations of some aromatic constituents. Noncarcinogenic risks higher > 1 indicate a non-negligible hazard to the population. The lifetime cancer risk due to PM_{10}-bound Cr was estimated to surpass the acceptable level. Relatively low cancer risks from the inhalation of PAHs were estimated. At the roadside, 78% of the samples were classified as toxic or very toxic, whereas the proportion was 57% at the background site. Toxicity was statistically correlated with OC, EC, anhydrosugars, PAHs and elements from exhaust and non-exhaust emissions. Traffic and biomass burning were found to be the major contributors to the overall toxicity of particulate matter. Thus, the adoption of mitigation measures focused on these sources is recommended. Awareness campaigns to educate end users on the best practices to operate wood combustion in the cleanest way are suggested. Political and financial support should be given to end-consumers to foster the replacement of the existing stock with modern and efficient biomass heating installations. Measures to promote cleaner modes of transportation should also be adopted.

CRediT authorship contribution statement

Célia Alves: Project administration, Funding acquisition, Conceptualisation, Methodology, Formal analysis, Supervision, Writing – original draft. Ismael Casotti Rienda: Investigation, Writing – review and editing. Ana Vicente: Investigation, Writing – review and editing. Estela Vicente: Investigation, Formal analysis, Writing – review and editing. Cátia Gonçalves: Investigation, Writing – review and editing. Carla Candeias: Investigation, Writing – review and editing. Franco Lucarelli: Investigation, Writing – review and editing. Giulia Pazzi: Investigation. Nora Kováts: Investigation, Writing – review and editing. Katalin Hubai: Investigation. Casimiro Pio: Investigation, Writing – review and editing. Oxana Tchepel: Project administration, Funding acquisition, Writing – review and editing.

Declaration of competing interest

The authors declare that they have no known competing financial interests or personal relationships that could have appeared to influence the work reported in this paper.

Acknowledgments

Ismael Casotti Rienda and Estela Vicente acknowledge the scholarships SFRH/BD/144550/2019 and SFRH/BD/117993/2016, respectively, from the Portuguese Foundation for Science and Technology (FCT). Ana Vicente was subsidised by national funds (OE), through FCT, I.P., in the framework contract foreseen in the numbers 4, 5 and 6 of article 23, of the Decree-Law 57/2016, of

August 29, changed by Law 57/2017, of July 19. We are also grateful for the support to CESAM (UIDB/50017/2020 + UIDP/50017/2020) and to GeoBioTec (UID/GEO/04035/2019 + UIDB/04035/2020), to FCT/MCTES through national funds, and co-funding by FEDER, within the PT2020 Partnership Agreement and Compete 2020. The sampling campaign was supported by the project "ISY-AIR: An integrated system for urban scale air quality assessment and forescast", MIT-EXPL/IRA/0023/2017, funded by FCT (MIT Portugal Program). The analytical work and toxicological bioassays were financially supported by the project "Chemical and toxicological SOurce PROfiling of particulate matter in urban air (SOPRO)", POCI-01-0145-FEDER-029574, funded by FEDER, through COMPETE2020 - Programa Operacional Competitividade e Internacionalização (POCI), and by national funds (OE), through FCT/MCTES. The *Vibrio fischeri* bioluminescent inhibition tests also had the support of the BIONANO_GINOP-2.3.2-15-2016-00017 project.

Appendix A. Supplementary data

Supplementary data to this article can be found online at https://doi.org/10.1016/j.atmosres.2021.xxxxx.

References

Almeida, S.M., Freitas, M.C., Repolho, C., Dionísio, I., Dung, H.M., Caseiro, A., Alves, C., Pio, C.A., Pacheco, A.M.G., 2009. Characterizing air particulate matter composition and sources in Lisbon, Portugal. J. Radioanal. Nucl. Chem. 281, 215-218. https://doi.org/10.1007/s10967-009-0113-8

Almeida, S.M., Pio, C.A., Freitas, M.C., Reis, M.A., Trancoso, M.A., 2005. Source apportionment of fine and coarse particulate matter in a sub-urban area at the Western European Coast. Atmos. Environ. 39, 3127-3138. https://doi.org/10.1016/j.atmosenv.2005.01.048

Almeida-Silva, M., Canha, N., Vogado, F., Baptista, P.C, Faria, A.V., Faria, T., Coutinho, J.T., Alves, C., Almeida, S.M., 2020. Assessment of particulate matter levels and sources in a street canyon at Loures, Portugal – a case study of the REMEDIO Project. Atmos. Pollut. Res. 11, 1857-1869. https://doi.org/10.1016/j.apr.2020.07.021

Alves, C., Nunes, T., Vicente, A., Gonçalves, C., Evtyugina, M., Marques, T., Pio, C., Bate-Epey, F., 2014. Speciation of organic compounds in aerosols from urban background sites in the winter season. Atmos. Res. 150, 57-68. https://doi.org/10.1016/j.atmosres.2014.07.012

Alves, C.A., Barbosa, C., Rocha, S., Calvo, A., Nunes, T., Cerqueira, M., Pio, C., Karanasiou, A., Querol, X., 2015a. Elements and polycyclic aromatic hydrocarbons in exhaust particles emitted by

light-duty vehicles. Environ. Sci. Pollut. Res. 22, 11526-11542. https://doi.org/10.1007/s11356-015-4394-x

Alves, C.A., Gomes, J., Nunes, T., Duarte, M., Calvo, A., Custódio, D., Pio, C., Karanasiou, A., Querol, X., 2015b. Size-segregated particulate matter and gaseous emissions from motor vehicles in a road tunnel. Atmos. Res. 153, 134-144.

Alves, C.A., Vicente, A.M., Custódio, D., Cerqueira, M., Nunes, T., Pio, C., Lucarelli, F., Calzolai, G., Nava, S., Diapouli, E., Eleftheriadis, K., Querol, X., Bandowe, B.A.M., 2017. Polycyclic aromatic hydrocarbons and their derivatives (nitro-PAHs, oxygenated PAHs, and azaarenes) in $PM_{2.5}$ from Southern European cities. Sci. Total Environ. 595, 494-504. https://doi.org/10.1016/j.scitotenv.2017.03.256

Alves, C.A., Vicente, A.M.P., Gomes, J., Nunes, T., Duarte, M., Bandowe, B.A.M., 2016. Polycyclic aromatic hydrocarbons (PAHs) and their derivatives (oxygenated-PAHs, nitrated-PAHs and azaarenes) in size-fractionated particles emitted in an urban road tunnel. Atmos. Res. 180, 128-137. https://doi.org/10.1016/j.atmosres.2016.05.013

Alves, C.A., Vicente, E.D., Evtyugina, M., Vicente, A.M., Nunes, T., Lucarelli, F., Calzolai, G., Nava, S., Calvo, A.I., Alegre, C.D., Oduber, F., Castro, A., Fraile, R., 2020a. Indoor and outdoor air quality: A university cafeteria as a case study. Atmos. Pollut. Res. 11, 531-544. https://doi.org/10.1016/j.apr.2019.12.002

Alves, C.A., Vicente, A.M.P., Calvo, A.I., Baumgardner, D., Amato, F., Querol, X., Pio, C., Gustafsson, M., 2020b. Physical and chemical properties of non-exhaust particles generated from wear between pavements and tyres. Atmos. Environ. 224, 117252. https://doi.org/10.1016/j.atmosenv.2019.117252

AQEG, 2019. Non-Exhaust Emissions from Road Traffic, Air Quality Expert Group, Department for Environment, Food and Rural Affairs, London. Available online: https://uk-air.defra.gov.uk/assets/documents/reports/cat09/1907101151_20190709_Non_Exhaust_Emissions_typeset_Final.pdf

Arif, A.T., Maschowski, C., Garra, P., Garcia-Käufer, M., Petithory, T., Trouvé, G., Dieterlen, A., Mersch-Sundermann, V., Khanaqa, P., Nazarenko, I., Gminski, R., Gieré. R., 2017. Cytotoxic and genotoxic responses of human lung cells to combustion smoke particles of Miscanthus straw, softwood and beech wood chips. Atmos. Environ. 163, 138-154. https://doi.org/10.1016/j.atmosenv.2017.05.019

Asheima, J., Vike-Jonas, K., Gonzalez, S.V., Lierhagen, S., Venkatramana, V., Veivåg, I.L., Snilsberg, B., Flaten, T.P., Asimakopoulos, A.G., 2019. Benzotriazoles, benzothiazoles and trace elements in an urban road setting in Trondheim, Norway: Re-visiting the chemical markers of traffic pollution. Sci. Total Environ. 649, 703-711. https://doi.org/10.1016/j.scitotenv.2018.08.299

Bandowe, B.A.M., Meusel, H., Huang, R., Ho, K., Cao, J., Hoffmann, T., Wilcke, W., 2014. $PM_{2.5}$-bound oxygenated PAHs, nitro-PAHs and parent-PAHs from the atmosphere of a Chinese

megacity: Seasonal variation, sources and cancer risk assessment. Sci. Total Environ. 473, 77-87. https://doi.org/10.1016/j.scitotenv.2013.11.108

Chalvatzaki, E., Chatoutsidou, S.E., Lehtomäki, H., Almeida, S.M., Eleftheriadis, K., Hänninen, O., Lazaridis, M., 2019. Characterization of human health risks from particulate air pollution in selected European cities. Atmosphere 10, 96. https://doi.org/10.3390/atmos10020096

Chang, S.H., Wang, Y.F., You, S.J., Kuo, Y.M., Tsai, C.H., Wang, L.C., Hsu, P.Y., 2013. Toxicity evaluation of fly ash by Microtox. Aerosol Air Qual. Res. 13, 1002-1008. https://doi.org/10.4209/aaqr.2012.10.0267

Cohen, A.J., Brauer, M., Burnett, R., Anderson, H.R., Frostad, J., Estep, K., Balakrishnan, K., Brunekreef, B., Dandona, L., Dandona, R., Feigin, V., Freedman, G., Hubbell, B., Jobling, A., Kan, H., Knibbs, L., Liu, Y., Martin, R., Morawska, L., Pope III, C.A., Shin, H., Straif, K., Shaddick, G., Thomas, M., van Dingenen, R., van Donkelaar, A., Vos, T., Murray, C.J.L., Forouzanfar, M.H., 2017. Estimates and 25-year trends of the global burden of disease attributable to ambient air pollution: an analysis of data from the Global Burden of Diseases Study 2015. Lancet 389, 1907-1918. https://doi.org/10.1016/S0140-6736(17)30505-6

Custódio, D., Cerqueira, M., Alves, C., Nunes, T., Pio, C., Esteves, V., Frosini, D., Lucarelli, F., Querol, X., 2016. A one-year record of carbonaceous components and major ions in aerosols from an urban kerbside location in Oporto, Portugal. Sci. Total Environ. 562, 822-833. https://doi.org/10.1016/j.scitotenv.2016.04.042

De Linares, C., Plaza, M.P., Valle, A., Alcázar, P., Guardia, C., Galán, C., 2021. Airborne Cupressaceae pollen and its major allergen, Cup a 1, in urban green areas of Southern Iberian Peninsula. Forests 12, 254. https://doi.org/10.3390/f12020254

Elzein, A., Stewart, G.J., Swift, S.J., Nelson, B.S., Crilley, L.R., Alam, M.S., Reyes-Villegas, E., Gadi, R., Harrison, R., Hamilton, J.F., Lewis, A.C., 2020. A comparison of $PM_{2.5}$-bound polycyclic aromatic hydrocarbons in summer Beijing (China) and Delhi (India). Atmos. Chem. Phys. 20, 14303-14319. https://doi.org/10.5194/acp-20-14303-2020

Gao, B., Wang, X.M., Zhao, X.Y., Ding, X., Fu, X.X., Zhang, Y.L., He, Q.F., Zhang, Z., Liu, T.Y., Huang, Z.Z., Chen, L.G., Peng, Y., Guo H., 2015. Source apportionment of atmospheric PAHs and their toxicity using PMF: Impact of gas/particle partitioning. Atmos. Environ. 103, 114-120. https://doi.org/10.1016/j.atmosenv.2014.12.006

Gerlofs-Nijland, M.E., Bokkers, B.G.H., Sachse, H., Reijnders, J.J.E., Gustafsson, M., Boere, A.J.F., Fokkens, P.F.H., Leseman, D.L.A.C., Augsburg, K., Cassee, F.R., 2019. Inhalation toxicity profiles of particulate matter: a comparison between brake wear with other sources of emission. Inhal. Toxicol. 31, 89-98. https://doi.org/10.1080/08958378.2019.1606365

Gonçalves, C., Alves, C., Fernandes, A.P., Monteiro, C., Tarelho, L., Evtyugina, M., Pio, C., 2011. Organic compounds in $PM_{2.5}$ emitted from fireplace and woodstove combustion of typical

Portuguese wood species. Atmos. Environ. 45, 4533-4545. https://doi.org/10.1016/j.atmosenv.2011.05.071

Gonçalves, C., Casotti Rienda, I., Nunes, T., Tchepel, O., Alves, C., 2021. PM_{10}-bound saccharides: chemical composition, sources and seasonal variations. Atmosphere 12, 194. https://doi.org/10.3390/atmos12020194

Grigoratos, T., Martini, G., 2014. Non-exhaust traffic related emissions. Brake and tyre wear PM. Literature review. Report EUR 26648 EN. Joint Research Centre. Publications Office of the European Union, Luxembourg. https://ec.europa.eu/jrc/en/publication/eur-scientific-and-technical-research-reports/non-exhaust-traffic-related-emissions-brake-and-tyre-wear-pm

Harrison, R.M., 2020. Airborne particulate matter. Phil. Trans. R. Soc. A 378, 20190319. https://doi.org/10.1098/rsta.2019.0319

He, J., Hu, Q., Jiang, M., Huang, Q., 2021. Nanostructure and reactivity of soot particles from open burning of household solid waste. Chemosphere 269, 129395. https://doi.org/10.1016/j.chemosphere.2020.129395

HEI, 2020. State of Global Air 2020. Special Report. Health Effects Institute. Boston, MA. https://www.stateofglobalair.org/

HSDB, 2020. Hazardous Substances Data Bank. National Center for Biotechnology Information, USA. https://pubchem.ncbi.nlm.nih.gov/

Kasurinen, S., Jalava, P.I., Happo, M.S., Sippula, O., Uski, O., Zimmermann, R., Jokiniemi, J., Koponen, H., Hirvonen, M., 2017. Particulate emissions from the combustion of birch, beech, and spruce logs cause different cytotoxic responses in A549 cells. Environ. Toxicol. 32, 1487-1499. https://doi.org/10.1002/tox.22369

Kazakos, V., Luo, Z., Ewart, I., 2020. Quantifying the health burden misclassification from the use of different $PM_{2.5}$ exposure Tier models: A case study of London. Int. J. Environ. Res. Public Health 17, 1099. https://doi.org/10.3390/ijerph17031099

Kelly, F.J., Fussell, J.C., 2015. Air pollution and public health: emerging hazards and improved understanding of risk. Environ. Geochem. Health 37, 631-649. https://doi.org/10.1007/s10653-015-9720-1

Kovacic, P., 2010. How dangerous are phthalate plasticizers? Integrated approach to toxicity based on metabolism, electron transfer, reactive oxygen species and cell signaling. Med. Hypotheses 74, 626-628. https://doi.org/10.1016/j.mehy.2009.11.032

Kováts, N., Ács, A., Kovács, A., Ferincz, Á., Turóczi, B., Gelencsér, A., 2012. Direct contact test for estimating the ecotoxicity of aerosol samples. Environ. Toxicol. Pharmacol. 33, 223-228. https://doi.org/10.1016/j.etap.2011.12.021

Låg, M., Øvrevik, J., Refsnes, M., Holme, J.A., 2020. Potential role of polycyclic aromatic hydrocarbons in air pollution-induced non-malignant respiratory diseases. Respir. Res. 21, Article number 299. https://doi.org/10.1186/s12931-020-01563-1

Lomnicki, S., Gullett, B., Stöger, T., Kennedy, I., Diaz, J., Dugas, T.R., Varner, K., Carlin, D., Dellinger, B., Cormier, S.A., 2014. Combustion by-products and their health effects - Combustion engineering and global health in the 21st century: Issues and challenges. Int. J. Toxicol. 33, 3-13. https://doi.org/10.1177/1091581813519686

Lucarelli, F., Calzolai. G, Chiari., Nava, S., Carraresi, L., 2018. Study of experience. Nucl. Instrum. Methods Phys. Res. B 417, 121-127. https://doi.org/10.1016/j.nimb.2013.05.099

Makar, M., Antonelli, J., , Q., Cutler, D., Schwartz, J., Dominici, F., 2017. Estimating the causal effect of low levels of fine particulate matter on hospitalization. Epidemiology 28, 627-634. https://doi.org/10.1097/ede.0000000000000690

Marconi, M., Sferlazzo, D.M., Becagli, S., Bommarito, C., Calzolai, G., Chiari, M., di Sarra, A., Ghedini, C., Gómez-Amo, J.L., Lucarelli, F., Meloni, D., Monteleone, F., Nava, S., Pace, G., Piacentino, S., Rugi, F., Severi, M., Traversi, R., Udisti, R., 2014. Saharan dust aerosol over the central Mediterranean Sea: PM_{10} chemical composition and concentration versus optical columnar measurements. Atmos. Chem. Phys. 14, 2039–2054. https://doi.org/10.5194/acp-14-2039-2014

Miller, M.R., 2020. Oxidative stress and the cardiovascular effects of air pollution. Free Radic. Biol. Med. 151, 69-87. https://doi.org/10.1016/j.freeradbiomed.2020.01.004

Nickovic, S., Vukovic, A., Vujadinovic, M., Djurdjevic, V., Pejanovic, G., 2012. Technical Note: High-resolution mineralogical database of dust-productive soils for atmospheric dust modeling. Atmos. Chem. Phys., 12, 845–855. https://doi.org/10.5194/acp-12-845-2012

Oliveira, C., Pio, C.A., Caseiro, A., Santos, P., Nunes, T., Mao, H., Luahana, L., Sokhi, R., 2010. Road Traffic Impact on urban Atmospheric Aerosol loading at Oporto, Portugal. Atmos. Environ. 44, 3147-3158. https://doi.org/10.1016/j.atmosenv.2010.05.027

Padoan, E., Amato, F., 2018. Vehicle Non-Exhaust Emissions: Impact on Air Quality. In: Non-Exhaust Emissions: An Urban Air Quality Problem for Public Health - Impact and Mitigation Measures. Amato, F. (Ed.), 2nd Chapter, pp. 21-65. Academic Press, London, UK.

Pankow, J.F., 1994a. An absorption model of gas/particle partitioning of organic compounds in the atmosphere. Atmos. Environ. 28, 185-188. https://doi.org/10.1016/1352-2310(94)90093-0

Pankow, J.F., 1994b. An absorption model of the gas/aerosol partitioning involved in the formation of secondary organic aerosol. Atmos. Environ. 28, 189-193. https://doi.org/10.1016/1352-2310(94)90094-9

Pardo, M., Katra, I., Schaeur, J.J., Rudich, Y., 2017. Mitochondria-mediated oxidative stress induced by desert dust in rat alveolar macrophages. GeoHealth 1, 4-16. https://doi.org/10.1002/2016gh000017

Perraudin, E., Budzinski, H., Villenave, E., 2007. Kinetic study of the reactions of ozone with polycyclic aromatic hydrocarbons adsorbed on atmospheric model particles. J. Atmos. Chem. 56, 57-82. https://doi.org/10.1007/s10874-006-9042-x

Pio, C., Alves, C., Nunes, T., Cerqueira, M., Lucarelli, F., Nava, S., Calzolai, G., Gianelle, V., Colombi, C., Amato, F., Karanasiou, A., Querol, X., 2020. Source apportionment of $PM_{2.5}$ and PM_{10} by Ionic and Mass Balance (IMB) in a traffic-influenced urban atmosphere, in Portugal. Atmos. Environ. 223, Article Number 117217. https://doi.org/10.1016/j.atmosenv.2019.117217

Pio, C., Cerqueira, M., Harrison, R., Nunes, T., Mirante, F., Alves, C., Oliveira, C., Sanchez de la Campa, A., Artíñano, B., Matos, M., 2011. OC/EC ratio observations in Europe: re-thinking the approach for apportionment between primary and secondary organic carbon. Atmos. Environ. 45, 6121-6132. https://doi.org/10.1016/j.atmosenv.2011.08.045

Poater, J., Duran, M., Solà, M., 2018. Aromaticity determines the relative stability of kinked vs. straight topologies in polycyclic aromatic hydrocarbons. Front. Chem. 6, 561. https://doi.org/10.3389/fchem.2018.00561

Puisney, C., Oikonomou, E.K., Nowak, S., Chevillot, A., Casale, S., Baeza-Squiban, A., Berret, J.F., 2018. Brake wear (nano)particle characterization and toxicity on airway epithelial cells *in vitro*. Environ. Sci. Nano 5, 1036-1044. https://doi.org/10.1039/C7EN00825B

Roux, M.V., Temprado, M., Chickos, J.S., Nagano, Y., 2008. Critically evaluated thermochemical properties of polycyclic aromatic hydrocarbons. J. Phys. Chem. Ref. Data 37, 1855-1996. https://doi.org/10.1063/1.2955570

Roy, D., Ahn, S.H., Lee, T.K., Seo, Y.C., Park, J., 2020. Cancer and non-cancer risk associated with PM_{10}-bound metals in subways. Transp. Res. D Transp. Environ. 89, 102618. https://doi.org/10.1016/j.trd.2020.102618

Sarkar, S., Khillare, P.S., 2013. Profile of PAHs in the inhalable particulate fraction: source apportionment and associated health risks in a tropical megacity. Environ. Monit. Assess. 185, 1199-1213. https://doi.org/10.1007/s10661-012-2626-9

Selley, L., Schuster, L., Marbach, H., Forsthuber, T., Forbes, B., Gant, T.W., Sandström, T., Camiña, N., Athersuch, T.J., Mudway, I., Kumar, A., 2020. Brake dust exposure exacerbates inflammation and transiently compromises phagocytosis in macrophages. Metallomics 12, 371-386. https://doi.org/10.1039/C9MT00253G

Slezakova, K., Morais, S., Pereira, M.C., 2014.Trace metals in size-fractionated particulate matter in a Portuguese hospital: exposure risks assessment and comparisons with other countries. Environ. Sci. Pollut. Res. 21, 3604-3620. https://doi.org/10.1007/s11356-013-2316-3

Stas, M., Aerts, R., Hendrickx, M., Delcloo, A., Dendoncker, N., Dujardin, A., Linard, S., Nawrot, T., Nieuwenhuyse, A.V., Aerts, J.M., Orshoven, J.V., Somers, B., 2021. Exposure to green space and pollen allergy symptom severity: A case-crossover study in Belgium. Sci. Total Environ. 781, 146682. https://doi.org/10.1016/j.scitotenv.2021.146682

Totlandsdal, A.I., Øvrevik, J., Cochran, R.E., Herseth, J.I., Bølling, A.K., Låg, M., Schwarze, P., Lilleaas, E., Holme, J.A., Kubátová, A., 2014. The occurrence of polycyclic aromatic

hydrocarbons and their derivatives and the proinflammatory potential of fractionated extracts of diesel exhaust and wood smoke particles. J. Environ. Sci. Health A Tox. Hazard Subst. Environ. Eng. 49, 383-396. https://doi.org/10.1080/10934529.2014.854586

USEPA, 2013. Users' Guide and Background Technical Document for USEPA Region 9 - Preliminary Remediation Goals (PRG) Table. https://semspub.epa.gov/work/02/103453.pdf

USEPA, 2017. Regional Screening Level (RSL) Summary Table. https://semspub.epa.gov/work/03/2245073.pdf

USEPA. 2019. IRIS Assessments. https://cfpub.epa.gov/ncea/iris2/atoz.cfm

Vicente, E.D., Vicente, A., Nunes, T., Calvo, A.I., del Blanco-Alegre, C., Oduber, F., Fraile, R., Amato, F., Alves, C., 2019. Household dust: loadings and PM_{10}-bound plasticizers and polycyclic aromatic hydrocarbons. Atmosphere 10, 785. https://doi.org/10.3390/atmos10120785

WHO, 2013. "Review of evidence on health aspects of air pollution – REVIHAAP Project" First results. World Health Organization Regional Office for Europe. Copenhagen, Denmark. https://www.ncbi.nlm.nih.gov/books/NBK361805/

Wu, G., Zhang, X., Zhang, C., Xu, T., 2016. Mineralogical and morphological properties of individual dust particles in ice cores from the Tibetan Plateau. J. Glaciol. 62, 46-53. https://doi.org/10.1017/jog.2016.8

Wu, W., Jin, Y., Carlsten, C., 2018. Inflammatory health effects of indoor and outdoor particulate matter. Clin. Rev. Allergy Immunol. 141, 833-844. https://doi.org/10.1016/j.jaci.2017.12.981

Xie, M., Barsanti, K.C., Hannigan, M.P., Dutton, S.J., Vedal, S., 2013. Positive matrix factorization of $PM_{2.5}$ - eliminating the effects of gas/particle partitioning of semivolatile organic compounds. Atmos. Chem. Phys. 13, 7381-7393. https://doi.org/10.5194/acp-13-7381-2013

Yadav, A., Behera, S.N., Nagar, P.K., Sharma, M., 2020. Spatio-seasonal concentrations, source apportionment and assessment of associated human health Risks of $PM_{2.5}$-bound polycyclic aromatic hydrocarbons in Delhi, India. Aerosol Air Qual. Res. 20, 2805-2825. https://doi.org/10.4209/aaqr.2020.04.0182

Zhang, J., Zhang, X., Wu, L., Wang, T., Zhao, J., Zhang, Y., Men, Z., Mao, H., 2018. Occurrence of benzothiazole and its derivates in tire wear, road dust, and roadside soil. Chemosphere 201, 310-317. https://doi.org/10.1016/j.chemosphere.2018.03.007

CRediT authorship contribution statement

Célia Alves: Project administration, Funding acquisition, Conceptualisation, Methodology, Formal analysis, Supervision, Writing – original draft. Ismael Casotti Rienda: Investigation, Writing – review and editing. Ana Vicente: Investigation, Writing – review and editing. Estela Vicente: Investigation, Formal analysis, Writing – review and editing. Cátia Gonçalves: Investigation, Writing – review and editing. Carla Candeias: Investigation, Writing – review and editing. Franco Lucarelli: Investigation, Writing – review and editing. Giulia Pazzi: Investigation. Nora Kováts: Investigation, Writing – review and editing. Katalin Hubai: Investigation. Casimiro Pio: Investigation, Writing – review and editing. Oxana Tchepel: Project administration, Funding acquisition Writing – review and editing.

Declaration of competing interest

The authors declare that they have no known competing financial interests or personal relationships that could have appeared to influence the work reported in this paper.

HIGHLIGHTS

Due to domestic wood combustion, PM_{10} levels in winter were twice as high as in spring

Traffic contribution to PM_{10} at the roadside was 7 times higher than at the background

Cancer risks resulting from exposure to PAHs by inhalation were estimated to be low

Noncarcinogenic risks higher > 1 indicate a non-negligible hazard to the population

Markers of biomass burning and traffic emissions correlated with toxicity